Rate Coefficients and Product Ion Distributions for Reactions of $CO_2 \cdot CO_2^+$ Ions with Neutral Molecules at 300 K

A. B. Rakshit and P. Warneck

Max-Planck-Institut für Chemie (Otto-Hahn-Institut), Mainz

Z. Naturforsch. **34a**, 1410–1423 (1979); received October 8, 1979

Reactions of $CO_2 \cdot CO_2^+$ ions with CO, N_2O, CH_4, H_2O, O_2, COS, C_2H_2, C_2H_4, C_3H_6, NH_3, CH_3NH_2, and NO have been studied using a drift tube mass spectrometer with selected ion injection. In most cases, the major reaction channel is charge transfer. Molecular displacement (switching) occurs also in several cases. In general, the measured rate coefficients agree with those calculated from Langevin or ADO theory. Two exceptions are the reactions with methylamine and nitric oxide where the rate coefficients are smaller by two orders of magnitude.

Introduction

Some time ago we described a drift chamber mass spectrometer technique for the investigation of reactions of cluster ions with neutral molecules [1]. This apparatus has now been employed to explore reactions of CO_2 dimer ions with a number of small neutral molecules, and the results are reported here. Several of these reactions were studied previously by Sieck [2], who used a quite different technique, so that data are available for comparison. Sieck has also pointed out the significance of $CO_2 \cdot CO_2^+$ reactions in electrical discharges [3], in the radiation chemistry of CO_2 [4], and in the lower ionospheres of the planets Mars and Venus [5]. We have studied $CO_2 \cdot CO_2^+$ reactions primarily to learn more about the fundamental behavior of this cluster ion.

Experimental

The apparatus has been described in detail previously [1, 6]. N_2^+ ions, produced by electron impact from nitrogen, are mass selected and then injected into a 16 mm deep reaction chamber filled with CO_2. Nearly thermal CO_2^+ ions are produced from N_2^+ by charge transfer in the vicinity of the injection point. $CO_2 \cdot CO_2^+$ are formed subsequently by third body attachment. A weak electric field (10 V/cm) drives these ions and any product ions resulting from reactions with added gases toward the rear plate of the reaction chamber, where they are sampled for mass spectrometric analysis. The secondary electron multiplier used previously as an ion detector was replaced by a channeltron followed by pulse counting circuity. The residence times of CO_2^+ and $CO_2 \cdot CO_2^+$ ions in the reaction chamber were determined as described previously [1, 6] by means of a pulsed ion beam-gating technique.

Carbon dioxide was freed from impurity oxygen by subjecting a small steel cylinder to cooling with liquid nitrogen and pumping volatile gases off. A complete elimination of water vapor impurity proved difficult, but its concentration was reduced sufficiently by passing CO_2 over phosphorus pentoxide. In addition, it was necessary to heat the inlet lines overnight to prevent an accumulation of residual water on the interior surfaces of the system. A dry ice cooled trap was also used as a precaution; the effect was minor, however, since the partial pressure of water vapor generally was much lower than the H_2O equilibrium vapor pressure at 195 K. The CO_2 flow and the chamber pressure were controlled by a servo leak valve. Research grade reactant gases were used without purification. They were mixed individually with excess CO_2 in a large glass vessel. From this reservoir the mixture was added to the CO_2 flow before it entered the reaction chamber. The partial pressure of reactant in the chamber was determined from the ratio of the two flow rates, the mixing ratio and the total chamber pressure. Flow rates were measured with Hastings-mass flow meters, all pressures were determined with diaphragm capacitance manometers. The total experimental and analysis error of these measurements amounts to about 20%.

Reprint requests to Prof. P. Warneck, Max-Planck-Institut für Chemie (Otto-Hahn-Institut), Saarstraße 23, D-6500 Mainz.

0340-4811 / 79 / 1200-1410 $ 01.00/0. — Please order a reprint rather than making your own copy.

Results and Discussion

a) Formation of CO_2 dimer Ions

Normalized intensities of CO_2^+ and its association product $CO_2 \cdot CO_2^+$ are shown in Fig. 1 as a function of CO_2 pressure. The decrease in intensity with increasing pressure is caused by reactions with water vapor leading to a variety of CO_2-water cluster ions. The summed intensities of all these ions constitute about 95% of the total intensity as shown by the dashed line in Figure 1. Thus, CO_2^+ is the predominant primary ion. About 3% of the total ion intensity is due to O_2^+ and $CO_2 \cdot O_2^+$, the remaining 2% consist of various impurity ions. O_2^+ and its association product $CO_2 \cdot O_2^+$ probably arises from O^+ ions formed as a byproduct in the initial N_2^+-CO_2 charge transfer process. The reaction $O^+ + CO_2 \rightarrow O_2^+ + CO$ is so rapid [7] that O^+ ions would not be observed at pressures of 0.2 torr or greater.

The determination of CO_2^+ residence times in the reaction chamber gave $\tau_{44} = 2.0 \cdot 10^{-4}\, p$ (sec) in the pressure range $0.2 < p < 0.4$ torr. The corresponding reduced mobility is $\mu_0(CO_2^+) = 1.04$ cm²/V sec. We have not found a literature value for the mobility of mass identified CO_2^+ at low electric fields with which our result might be compared. Saporoschenko [8] has determined mobilities of

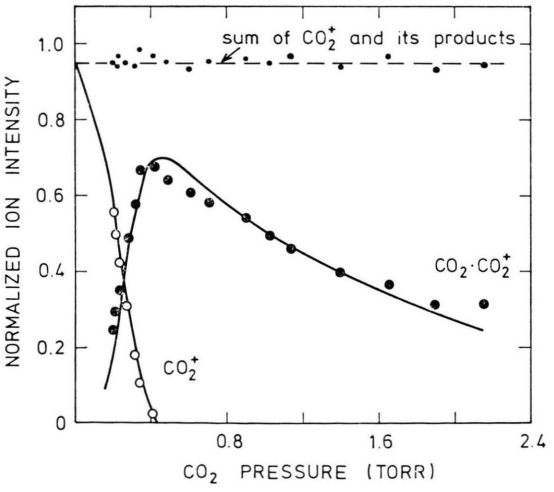

Fig. 1. Formation of CO_2 dimer ions as a function of CO_2 pressure. The decrease of $CO_2 \cdot CO_2^+$ intensity with rising pressure is due to reaction with H_2O impurity. The sum of CO_2^+, $CO_2 \cdot CO_2^+$ and products from their reactions is shown by the dashed line.

CO_2^+ at reduced field strengths $E/p > 50$ V/cm torr. By extrapolation to low fields he derived $\mu_0(CO_2^+) = 1.13$ cm²/V sec. Low field mobilities for several other ions in CO_2 are known, e.g. $\mu_0(O_2^+) = 1.35$ cm²/V sec [8, 9] and $\mu_0(CO_3^-) = 1.27$ cm²/V sec [9, 10]. Compared with these values, the mobility of CO_2^+ is much lower. This behavior is expected, since for an ion moving in its parent gas resonant charge transfer would dominate the collisional interaction. Knowing the CO_2^+ ion residence time, we derive from the decrease of CO_2^+ ion intensity with pressure the rate coefficient for the reaction

$$CO_2^+ + CO_2 \rightarrow CO_2 \cdot CO_2^+ + CO_2 \,. \qquad (1)$$

The averaged value obtained using all data points, $k_1 = 2.8 \cdot 10^{-28}$ cm⁶/molecule sec is in good agreement with previous determinations [2, 11]. The data indicate a trend, however, which we interpret to derive from the parallel reaction

$$CO_2^+ + H_2O \qquad (2)$$

HCO_2^+, H_2O^+, neutral products.

When this reaction is included one must write for the decrease of CO_2^+ ion intensity

$$I_{44} = 0.95 \exp[-(k_1 n_M^2 + k_2 n_1)\tau_{44}]$$
$$= 0.95 \exp[-k_1 n_M^2 (1 + a/p^2)\tau_{44}], \quad (A)$$

where n_M and n_1 are the number densities of CO_2 and H_2O, respectively, and $a = k_2 n_1 / k_1 \gamma^2$ with $\gamma = 3.25 \cdot 10^{16}$ particles/cm³ arising from the conversion of number density to pressure. The above equation suggests a linear increase of the effective rate coefficient with $1/p^2$ and, as Fig. 2 shows this relation is indeed observed. The true rate coefficient k_1 is obtained by extrapolation to the ordinate: $k_1 = 2.1 \cdot 10^{-28}$ cm⁶/molec sec. This result is preferred over that noted above.

One now calculates that the conversion of CO_2^+ to $CO_2 \cdot CO_2^+$ is essentially complete within one tenth of the total CO_2^+ drift path in the reaction chamber at pressures greater than 0.81 torr. At greater pressures, $CO_2 \cdot CO_2^+$ may be treated as a primary ion. The residence time of $CO_2 \cdot CO_2^+$ in the reaction chamber was determined as $\tau_{88} = 1.75 \cdot 10^{-4}\, p$(sec) in the pressure range $0.85 < p < 2.2$ torr. The corresponding reduced mobility is $\mu_0(CO_2 \cdot CO_2^+) = 1.19$ cm²/V sec and this value is in good agreement with the estimate of $\mu_0 = 1.22$ cm³/V sec obtained by Smith et al. [12] by means

of a scaling procedure using the known mobility of CO_3^-.

The behavior of $CO_2 \cdot CO_2^+$ ion intensity as a function of pressure is determined by its formation via reaction (1) and by its loss due to reaction

$$CO_2 \cdot CO_2^+ + H_2O \rightarrow \text{products}. \qquad (3)$$

A general mathematical treatment of the processes taking place in the reaction chamber and formulae for the intensities of product ions emerging from the exit aperture of the chamber have been given previously [1]. In the present application one finds

$$I(88) = \frac{0.95}{x - (1 + a/p^2)} \cdot (\exp[-k_1(1 + a/p^2)\, n_M{}^2\, \tau_{44}] - \exp[-k_1\, n_M{}^2\, X\, \tau_{44}]), \qquad (B)$$

with $X = k_3 n_1 \mu_{44}/k_1 n_M{}^2 \mu_{44}$. The ratio of mobilities $\mu_{44}/\mu_{88} = 0.874$ is obtained from the measurements of residence times. The solid lines in Fig. 1 are calculated with the value $a = 0.021$ derived from Fig. 2 and $k_3 n_1 = 3.6 \cdot 10^3\ \text{sec}^{-1}$. The rate coefficient k_3 has been determined in a separate experiment which will be described later.

In the study of reactions of $CO_2 \cdot CO_2^+$ ions the chamber pressure was held constant at about 0.85 torr. This choice of pressure was a compromise between minimizing the loss of dimer ions due to reactions with water impurity and a conversion of CO_2^+ ions to $CO_2 \cdot CO_2^+$ at as small a distance from the injection aperture as was possible.

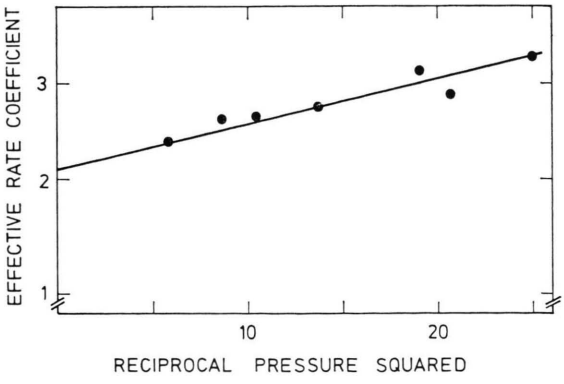

Fig. 2. Plot of experimental rate coefficient k_1 for the CO_2^+-CO_2 association reaction versus the square of reciprocal pressure. Extrapolation to the ordinate gives the true termolecular rate coefficient.

b) Evaluation of Data for $CO_2 \cdot CO_2^+$ Reactions

At pressure of about 0.85 torr, the effect of reaction (2) is almost negligible and $X \approx 1$ so that Eq. (B) simplifies to one exponential term. The addition of a neutral reactant with density n_R causes the $CO_2 \cdot CO_2^+$ to decrease according to

$$I(88)\, 0.95 \exp[-(k_3 n_1 + k_R n_R)\, \tau_{88}] = I_0(88) = \exp(-k_R n_R \tau_{88}). \qquad (C)$$

Here, $I_0(88)$ is the dimer ion intensity in the absence of a reactant and k_R, the rate coefficient for the reaction, can be obtained directly from the exponential decay of $I(88)$ with increasing n_R in the usual manner. The treatment of product ion intensities is somewhat more involved because on one hand more than one product channel exists in several reactions and, on the other hand, the product ions frequently enter into secondary reactions leading to new products. Equations describing the product ion intensities thus depend on the details of the reaction mechanisms by which the products are assumed to arise. Examples for equations describing product ion intensities for a variety of mechanisms are contained in previous papers [1, 6, 13]. To conserve space, we shall not list detailed formulae for the various reaction mechanisms. Equations are derived stepwise by integration of the kinetic equations for the ion densities as a function of drift distance in the reaction chamber, taking into account that each ion moves with its own speed. Rate coefficients in the integrated equations are thus weighted with the ratios of ion mobilities. Since experimental values for mobilities are available only for a few ions, we assume that the mobilities are inversely proportional to the root of the reduced mass of the collision pair ion–CO_2. The known mobilities for $CO_2 \cdot CO_2^+$ and O_2^+ in CO_2 are taken as reference values. This assumption corresponds to classical mobility theory and has been used also by others [12]. The rate coefficients appearing in the equations for product ion intensities and the branching ratios for reactions yielding more than one product were treated as parameters. These were determined by seeking the best fit of the calculated ion intensities to the experimental data. It should be noted that the total product ion intensity may exceed the initial intensity of CO_2 dimer ions because the extent of the $CO_2 \cdot CO_2^+ + H_2O$ reaction is increasingly suppressed as the density n_R of added reactant is raised.

c) Individual $CO_2 \cdot CO_2^+$ Reactions

Table 1 summarizes product distributions and rate coefficients for the various CO_2 dimer reactions studied. Results inferred for several related reactions required to explain the observed secondary products are compiled in Table 2. The individual results will be described in more detail below. Values for rate coefficients are given in units of cm^3, molecules, and sec with powers of ten indicated in parentheses.

Table 1. Product distribution and rate coefficients for reactions of $CO_2 \cdot CO_2^+$ ions.

Reaction No.	Reactant	Ionization potential [a]	Product distribution (%)	k_{exp} [b]	k_{ADO} [b]	Previous data [c]
4	CO	14.0	$CO_2 \cdot CO^+$ (100)	2.8	7.1	2.2
5	N_2O	12.89	N_2O^+ ($\geqq$ 90), $CO_2 \cdot N_2O^+$ ($\leqq$10)	7.5	7.4	6.7
6	CH_4	12.70	CH_3CO^+ (5), CH_4^+ (95) or $(CO_2)_2H^+$ (90), $CO_2 \cdot CH_4^+$ (5) [d]	5.8	10.3	3.8
3	H_2O	12.60	probably H_2O^+, $CO_2 \cdot H_2O^+$	16	18.3	
7	SO_2	12.34	SO_2^+ ($\geqq$ 30), $CO_2 \cdot SO_2^+$ ($\geqq$ 70)	13	12.6	
8	O_2	12.06	O_2^+ (85), $CO_2 \cdot O_2^+$ (15)	1.8	6.0	1.5
9	COS	11.17	COS^+ ($\geqq$ 90), $CO_2 \cdot COS^+$ ($\geqq$ 10)	11	10.4	
10	C_2H_2	11.40	$C_2H_2^+$ ($\geqq$ 77), $CO_2 \cdot C_2H_2^+$ ($\leqq$ 23)	7.0	9.5	4.3
11	C_2H_4	10.45	$C_2H_4^+$ (100)	13.5	10.5	
12	C_3H_6	9.74	$C_3H_6^+$ (52, $C_3H_5^+$ (40), $C_3H_4^+$ (8)	20.5	10.8	
13	NH_3	10.17	NH_3^+ ($\geqq$ 50), $CO_2 \cdot NH_3^+$ ($\leqq$ 50)	6.0	17.1	
14	CH_3NH_2	8.97	NH_3^+ (48), NH_4^+ (9), $CH_3NH_3^+$ (43) [d]	0.017	14.2	
15	NO	9.25	—	0.01	6.5	

[a] From the compilation of Ref. [33] (in eV).
[b] In units of 10^{-10} cm^3/molecule sec.
[c] W. L. Sieck, Ref. [2].
[d] Includes secondary products.

Table 2. Miscellaneous reactions occurring in conjunction with reactions of $CO_2 \cdot CO_2^+$ ions.

No.	Reaction		$k_{deduced}$ [a]	k_{ADO} [a]
1	$CO_2^+ + 2\,CO_2$	$\rightarrow CO_2 \cdot CO_2^+ + CO_2$	2.1 (— 28)	—
2	$CO_2^+ + H_2O$	$\rightarrow$ Products [b]	2.1 (— 9)	2.1 (— 9)
16	$CO_2 \cdot CO^+ + CO$	$\rightarrow CO \cdot CO^+ + CO_2$	3.3 (— 10)	7.3 (— 10)
17	$CO_2 \cdot CO^+ + 2\,CO_2$	$\rightarrow (CO_2)_2 \cdot CO^+ + CO_2$	6.5 (— 30)	—
19	$N_2O^+ + 2\,CO_2$	$\rightarrow N_2O^+ \cdot CO_2 + CO_2$	~7 (— 30)	—
20	$N_2O^+ + N_2O + CO_2$	$\rightarrow N_2O \cdot N_2O^+ + CO_2$	~7 (— 27)	—
25	$O_2^+ + 2\,CO_2$	$\rightarrow CO_2 \cdot O_2^+ + CO_2$	1.2 (— 29)	—
26	$CO_2 \cdot O_2^+ + 2\,CO_2$	$\rightarrow (CO_2)_2 \cdot O_2^+ + CO_2$	~1 (— 30)	—
28	$CO_2 \cdot COS^+ + COS$	$\rightarrow (COS)_2^+ + CO_2$	~3 (— 10)	1.0 (— 10)
29	$COS^+ + COS + CO_2$	$\rightarrow (COS)_2^+ + CO_2$	~5 (— 27)	—
30	$COS^+ + 2\,CO_2$	$\rightarrow CO_2 \cdot COS^+ + CO_2$	$\leqq$2 (— 30)	—
31	$C_2H_2^+ + 2\,CO_2$	$\rightarrow CO_2 \cdot C_2H_2^+ + CO_2$	$\leqq$4 (— 30)	—
32	$C_2H_2^+ + C_2H_2$	$\rightarrow$ Products [b]	1.4 (— 9)	1.2 (— 9)
32a	$C_2H_2^+ + C_2H_2^+ + CO_2$	$\rightarrow (C_2H_2)_2^+ + CO_2$	1.6 (— 26)	—
33	$CO_2 \cdot C_2H_2^+ + C_2H_2$	$\rightarrow (C_2H_2)_2^+ + CO_2$	0.3—1 (— 9)	9.8 (— 10)
34	$(C_2H_2)_2^+ + C_2H_2 + CO_2$	$\rightarrow (C_2H_2)_3^+ + CO_2$	7.6 (— 27)	—
35	$C_4H_3^+ + C_2H_2 + CO_2$	$\rightarrow C_4H_3^+ \cdot C_2H_2 + CO_2$	1.5 (— 26)	—
36	$C_4H_2^+ + C_2H_2 + CO_2$	$\rightarrow C_4H_2^+ \cdot C_2H_2 + CO_2$	2.3 (— 26)	—
37—38	$C_2H_4^+ + C_2H_4$	$\rightarrow C_3H_5^+ + CH_3$	1.4 (— 10)	1.3 (— 9)
39	$C_2H_4^+ + C_2H_4 + CO_2$	$\rightarrow (C_2H_4)_2^+ + CO_2$	6.3 (— 26)	—
40a	$C_3H_6^+ + C_3H_6 + CO_2$	$\rightarrow (C_3H_6)_2^+ + CO_2$	4.4 (— 26)	—
40	$C_3H_6^+ + C_3H_6$	$\rightarrow$ Products [b]	2.1 (— 9)	1.3 (— 9)
41a	$C_3H_5^+ + C_3H_6 + CO_2$	$\rightarrow C_6H_{11}^+ + CO_2$	6.4 (— 26)	—
41	$C_3H_5^+ + C_3H_6$	$\rightarrow$ Products [b]	2.1 (— 9)	1.3 (— 9)
42	$C_3H_4^+ + C_3H_6$	$\rightarrow$ Products [b]	1.6 (— 9)	1.3 (— 9)
43	$(C_3H_6)_2^+ + C_3H_6 + CO_2$	$\rightarrow (C_3H_6)_3^+ + CO_2$	1.1 (— 26)	—
44	$NH_3^+ + 2\,CO_2$	$\rightarrow CO_2 \cdot NH_3^+ + CO_2$	$\leqq$2 (— 29)	—
45	$NH_3^+ + NH_3$	$\rightarrow NH_4^+ + NH_2$	1.3 (— 9)	2.2 (— 9)
46	$CO_2 \cdot NH_3^+ + NH_3$	$\rightarrow$ Products [b]	8.5 (— 10)	1.8 (— 9)

[a] In units of cm^3/molec sec for bimolecular reactions, cm^6/$molec^2$ sec for termolecular reactions, powers of ten given in parentheses.
[b] See text.

Carbon Monoxide (I.P. 14.0 eV)

The behavior of reactant and product ion intensities as a function of CO partial pressure is shown in Figure 3. The only primary product ion is $CO_2^+ \cdot CO$. Charge transfer would be endoergic, since the ionisation energy of CO exceeds that of CO_2. The rate coefficient found for the reaction $k_4 = 2.8\,(-10)$ is in good agreement with the recent value $2.2\,(-10)$ obtained by Sieck [2]. Assuming that $CO_2^+ \cdot CO$ enters the subsequent reactions

$$CO_2^+ \cdot CO + CO \rightarrow CO \cdot CO^+ + CO_2\,, \qquad (16)$$

$$CO_2^+ \cdot CO + 2\,CO_2 \rightarrow (CO_2)_2^+\,CO + CO_2 \qquad (17)$$

we calculate the solid lines in Fig. 3 with $k_{16} = 3.3\,(-10)$ and $k_{17} = 6.5\,(-30)$. Sieck [2] reported for these reactions the rate coefficients: $2.0\,(-10)$ and $1.4\,(-31)$, respectively. Reaction (17) thus seems to be more efficient than was thought previously.

Nitrous Oxide (I.P. 12.89 eV)

Very small amounts of N_2O introduced to the reaction chamber caused the CO_2 dimer ion intensity to decay rapidly. Essentially equivalent intensities of N_2O^+ were produced indicating that at least 90% of the reaction occurs by charge transfer. The rate coefficient as obtained from the initial slope is $k_5 = 8.2\,(-10)$. This value requires a downward correction owing to H_2O and O_2 impurities contained in the N_2O as explained further below. The corrected rate coefficient is $k_5 = 7.5\,(-10)$. This is in agreement with Sieck's result [2] of $6.7\,(-10)$ at similar CO_2 pressures and also with average dipole orientation (ADO) theory [14] which predicts $7.4\,(-10)$. At higher N_2O partial pressures the mass 88 ion intensity approaches an almost constant value and the N_2O^+ intensity decreases. These data were not very reproducible and depended on the extent to which water impurity was present. Typical results are shown in Fig. 4. At least three reactions must be considered to explain the decay of N_2O^+ intensity with rising N_2O partial pressure.

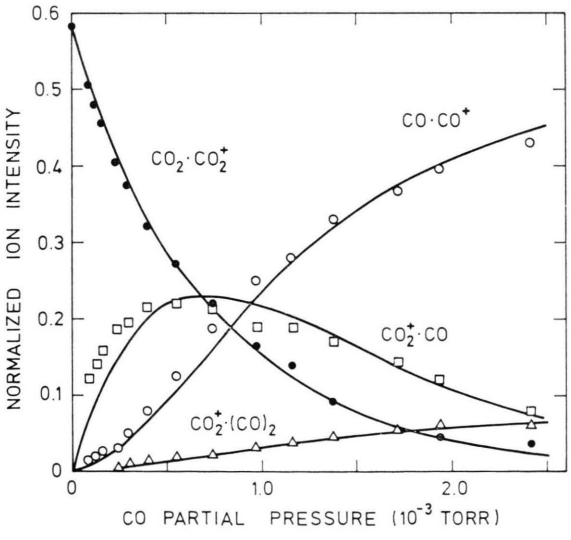

Fig. 3. Decay of CO_2 dimer ion intensity and rise of product ion intensities due to reaction $CO_2 \cdot CO_2^+$ with CO Solid lines calculated as described in the text.

$$N_2O^+ + H_2O \rightarrow H_2O^+ + N_2O\,, \qquad (18)$$

$$N_2O^+ + 2\,CO_2 \rightarrow N_2O^+ \cdot CO_2 + CO_2\,, \qquad (19)$$

$$N_2O^+ + N_2O + CO_2 \rightarrow N_2O \cdot N_2O^+ + CO_2\,. \qquad (20)$$

The first of these is required to account for the sizable increase of the intensities of water cluster ions. The other two reactions give products having the same mass as the $CO_2 \cdot CO_2^+$ ion and these must be responsible for the behavior of mass 88 ion intensity at higher N_2O pressures. Both $N_2O^+ \cdot CO_2$ and $N_2O \cdot N_2O^+$ will also undergo reactions with H_2O. We have assumed rate coefficients for these reactions and reaction (18) of $1.6\,(-9)$, equal to that for the reaction $CO_2 \cdot CO_2^+ + H_2O$ (see below). Irrespective of their nature, the water product ions from these reactions and H_2O^+ from reaction (18) will enter into the chain of reactions giving the observed array of H_2O cluster ions. Since the individual reaction steps are not known we have, for simplicity, summed all H_2O ion intensities. The amount of water vapor present in the absence of N_2O was found to be below that needed to account for all of the observed water ion intensity, therefore, it appears that an additional small amount of H_2O is carried into the chamber together with the N_2O. The sum of the ion intensities of O_2^+, $CO_2 \cdot O_2^+$ and $H_2O \cdot O_2^+$ also rose with increasing N_2O pressure, so that some oxygen impurity seemed to be carried in as well. The intensities of oxygen related ions were added to those of the water related ions and the sum is shown in Fig. 4 by the triangles. The oxygen ions constitute about 10% of the total impurity ion intensity. If the rate coefficient for the reaction $N_2O^+ + O_2$ is estimated to be a factor of ten smaller than that

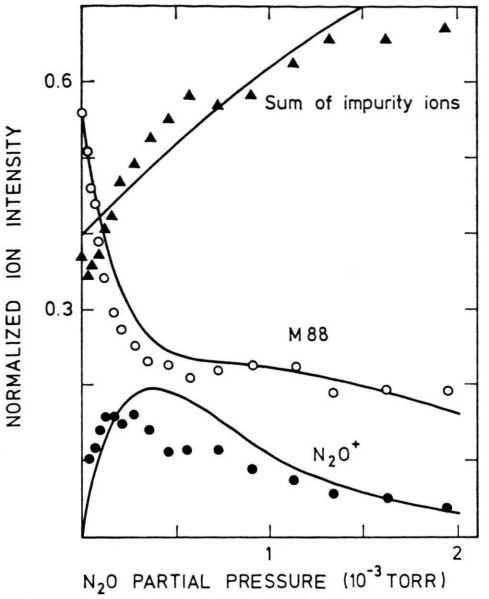

Fig. 4. Behavior of mass 44 and 88 ion intensities as a function of N_2O partial pressure. Triangles give the sum of intensities of water cluster ions and oxygen related ions. Solid lines were calculated as described in the text.

for the reaction $N_2O^+ + H_2O$, the O_2 impurity partial pressure will about equal that of water vapor. On this premise, we have tried to model the behavior of ion intensities. The solid lines in Fig. 4 were calculated using $k_{19} = 7.5\,(-30)$, $k_{20} = 7.5\,(-27)$ and a ratio of water vapor plus oxygen to N_2O partial pressure of 0.075. A particularly good fit is not obtained, but the main features of the behavior of the ion intensity are reproduced. It should be noted that the rate coefficient k_{19} shapes the N_2O^+ and mass 88 ion intensities at N_2O partial pressures below $4 \cdot 10^{-4}$ torr, but has little influence on the mass 88 intensity at higher N_2O pressures. In this pressure domain, the ion intensities are affected mainly by k_{19}. The value of k_{20} needed to reproduce the data is fairly high, but there is little latitude for a better fit of the data using a much smaller value. This finding points towards interesting differences in the effectivity of third body association between N_2O^+ and CO_2^+ in carbon dioxide. Both ions and, of course, their neutral parent molecules are isoelectronic and are generally assumed to behave rather similarly. And yet the third body association of N_2O^+ with CO_2 is by at least an order of magnitude slower than that of CO_2^+ with CO_2, whereas the association of N_2O with N_2O in CO_2 seems to proceed ten times faster. Note, however, that for the association of N_2O^+ with N_2O in nitrous oxide a rate coefficient of $4.8\,(-28)$ has been reported [15]; it is difficult to understand why replacing N_2O by CO_2 as the third body should increase the rate of $N_2O \cdot N_2O^+$ formation by an order of magnitude. Independent experiments are thus needed to resolve this problem.

Methane (I.P. 12.70 eV)

Results for the reaction of CO_2 dimer ions with methane are shown in Figure 5. The rate coefficient for this reaction is determined as $k_6 = 5.8\,(-10)$, whereas Sieck [2] reported $3.8\,(-10)$. The major product is $(CO_2)_2H^+$. Minor products are $CO_2 \cdot CH_4^+$. The last ion was identified previously by Sieck [2]. He reported a branching ratio $CH_3CO^+/(CO_2)_2H^+ = 0.33$ independent of pressure in the range 0.4—0.9 torr. We find a ratio 0.06 at 0.85 torr. The formation of CH_3CO^+ as a product ion from reaction (6) clearly involves a major rearrangement of the intermediate reaction complex, but the present data give us clues to the details of the CH_3CO^+ formation mechanism. The solid lines in Fig. 5 were calculated assuming that the three observed products derive directly from reaction (6) with the probabilities 0.9 for $(CO_2)_2H^+$ and 0.05 each for $CO_2 \cdot CH_4^+$ and CH_3CO^+.

The intensities of $(CO_2)_2H^+$ and $CO_2 \cdot CH_4^+$ may be explained equally well by an alternative mechanism, in which charge transfer rather than hydrogen

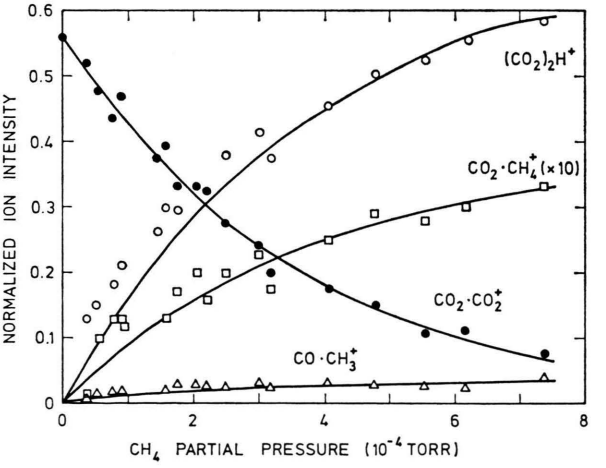

Fig. 5. Reactant and product ion intensities for the reaction of CO_2 dimer ions with methane. Solid lines were calculated as described in the text.

abstraction provides the dominant channel of reaction (6):

$$CO_2 \cdot CO_2^+ + CH_4 \rightarrow CH_4^+ + 2\,CO_2\,, \quad (6a)$$
$$CH_4^+ + CO_2 \rightarrow (CO_2 \cdot CH_4^+)^*\,, \quad (21)$$
$$(CO_2 \cdot CH_4^+)^* \rightarrow CO_2H^+ + CH_3\,, \quad (22)$$
$$(CO_2 \cdot CH_4^+)^* + CO_2 \rightarrow CO_2 \cdot CH_4^+ + CO_2\,, \quad (23)$$
$$CO_2H^+ + 2\,CO_2 \rightarrow (CO_2)_2H^+ + CO_2\,. \quad (24)$$

In this mechanism the formation of $CO_2 \cdot CH_4^+$ occurs by collisional stabilization of the intermediate reaction complex $(CO_2 \cdot CH_4^+)^*$ rather than via the displacement channel in reaction (6).

The reaction sequence (21) and (22) leading to the intermediate product CO_2H^+ has been investigated by Harrison and Blair [16] by means of pulsed source mass spectrometry and a rate coefficient $k_{21-22} = 1.2\,(-9)$ was obtained. The reaction is so rapid that CH_4 ions would not be observed in our experiments. On the other hand, a signal at mass number 45, corresponding to CO_2H^+ has been observed with about 1% of the total ion intensity. This magnitude is calculated to be consistent with the outlined mechanism provided the rate coefficient for the association reaction (24) is $k_{24} \approx 1\,(-28)$. Unless this rate coefficient is demonstrated to be much smaller we are inclined to believe that this second mechanism applies.

Water Vapor (I.P. 12.6 eV)

From the exponential decrease of CO_2 dimer ion intensity with increasing H_2O flow we determine the rate coefficient associated with reaction (3) as $k_3 = 1.6\,(-9)$. This value may represent a lower limit because of the possibility that after preparing the H_2O/CO_2 mixture losses of water occurred on the walls of the mixing vessel or the inlet line leading to the reaction chamber. The products expected from this reaction are either H_2O^+ or $CO_2 \cdot H_2O^+$, or both. A signal at mass number 18 was not detected. The M 62 signal already present from the water impurity did also not rise significantly when the H_2O concentration was increased. The most prominent increase occurred at M 37 corresponding to the ion $H_3O^+ \cdot H_2O$. This ion certainly is a secondary product. The route to its formation cannot be deduced from this experiment.

The rate coefficient k_3 can be used to calculate the density of impurity water vapor from the quantity $k_3 n_1 = 3.6 \cdot 10^3$ derived earlier from Figure 1. One finds $n_1 = 2.2 \cdot 10^{12}$ cm^{-3} corresponding to a vapor pressure of about $7 \cdot 10^{-5}$ torr. The rate coefficient for the reaction CO_2^+ with water vapor is then determined from the value for $a = k_2 n_1 / k_1 \gamma^2$ which was obtained from the slope of the straight line in Fig. 2 as $a = 0.021$. The result is $k_2 = 2.1\,(-9)$, a value in good agreement with the recent determination by Karpas, Anicich and Huntress [17] who employed the ion cyclotron resonance technique and found $k_2 = 2.8\,(-9)$. ADO theory predicts $k_2 = 2.3\,(-9)$.

Sulfur Dioxide (I.P. 12.34 eV)

Detailed results for this rapid reaction were reported elsewhere [18]. Both charge transfer and molecular displacement products were found. The data are entered in Table 1 for comparison with the other reactions.

Oxygen (I.P. 12.06 eV)

Normalized ion intensities observed upon the addition of oxygen to the reaction chamber are displayed in Figure 6. The rate coefficient for the reaction, obtained from the exponential decay of $CO_2 \cdot CO_2^+$ ion intensity as a function of O_2 partial pressure is $k_8 = 1.85\,(-10)$. This may be compared with a value of $1.5\,(-10)$ reported by Sieck [2]. The reaction appears to proceed both by charge transfer and by molecular displacement, but the formation of $CO_2 \cdot O_2^+$ by third body association from O_2^+ must also be included:

$$CO_2 \cdot CO_2^+ + O_2 \xrightarrow{a} O_2^+ + 2\,CO_2$$
$$\xrightarrow{b} CO_2 \cdot O_2^+ + CO_2\,, \quad (8)$$
$$O_2^+ + 2\,CO_2 \rightarrow CO_2 \cdot O_2^+ + CO_2\,. \quad (25)$$

Adams et al. [19] reported $k_{25} = 2.3\,(-29)$ from flowing afterglow experiments at 200 K for Helium as carrier gas, whereas Sieck [2] gives $4.6\,(-30)$ at 300 K for CO_2 as the third body. If one assumes that O_2^+ is the only product from reaction (8), a rate coefficient of $k_{25} = 1.4\,(-29)$ is required to approximately represent the O_2^+ ion intensities in Figure 6. On the other hand, if Sieck's value for k_{25} is employed the O_2^+ ion intensity is well represented with $k_{8a}/k_8 = 0.6$.

The observation of O_2^+ in CO_2 free from oxygen provides an opportunity for an independent determination of k_{25}. Figure 7 shows intensities for O_2^+ and $CO_2 \cdot O_2^+$ obtained as a function of CO_2 pressure in the absence of additional reactants. The

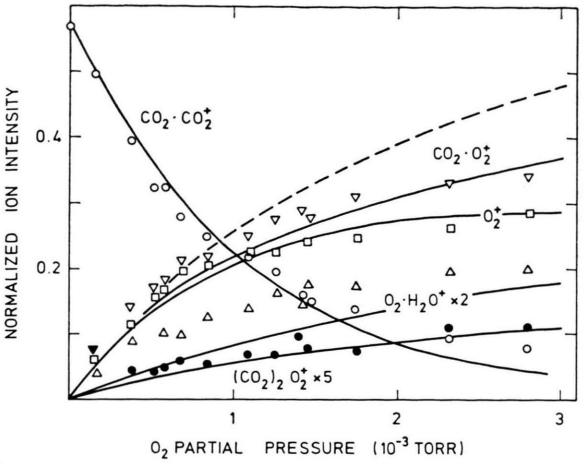

Fig. 6. Reactant and product ion intensities for the reaction of CO_2 dimer ions with oxygen. Solid lines were calculated as described in the text. The dashed line gives the calculated $CO_2 \cdot O_2^+$ ion intensity for the case that this ion does not undergo a subsequent reaction with H_2O impurity.

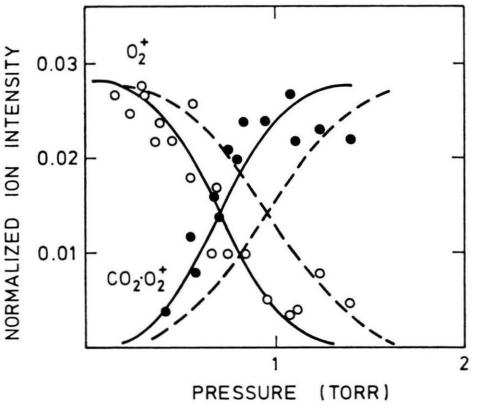

Fig. 7. Behavior of ion intensities at mass 32 (open circles) and mass 76 (filled circles) as a function of CO_2 pressure in the reaction chamber. Solid lines were calculated with a rate coefficient for O_2^+-CO_2 association $k_{25} = 1.2$ (− 29). Dashed lines result from a similar calculation with $k_{25} = 5$ (− 30) as given by Sieck [2].

data points show a greater scatter owing to the fairly low ion intensities, but the conversion of O_2^+ to $CO_2 \cdot O_2^+$ with increasing pressure is well documented. If we assume that O_2^+ is formed near the entrance orifice to the reaction chamber (due to the process $O^+ + CO_2$) and assign a residence time for O_2^+ ions $\tau_{32} = 1.54 \cdot 10^{-4}\, p$ sec consistent with their known reduced mobility [9] of $\mu_0 = 1.35$ cm²/V sec, we find that the data in Fig. 7 are well represented with $k_{25} = 1.2$ (− 29). This is indicated by the solid lines. For comparison, the dashed lines were calculated on the basis $k_{25} = 5$ (− 30). We have used our value, $k_{25} = 1.2$ (− 29), to calculate O_2^+, $CO_2 \cdot O_2^+$ and other ion intensities as a function of O_2 partial pressure in Figure 6. These are shown by the solid lines. The required channel probability for O_2^+ formation in reaction (8) is 0.85. The observed $CO_2 \cdot O_2^+$ ion intensity turns out to be lower than calculated, if this ion were unreactive. Since $(CO_2)_2O_2^+$, $O_2 \cdot H_2O^+$ and $CO_2 \cdot O_2 \cdot H_2O^+$ occur as product ions we have considered the additional reactions

$$CO_2 \cdot O_2^+ + 2\,CO_2 \rightarrow (CO_2)_2O_2^+ + CO_2\,, \quad (26)$$

$$CO_2 \cdot O_2^+ + H_2O \rightarrow O_2 \cdot H_2O^+ + CO_2\,, \quad (27)$$

and assume that $CO_2 \cdot O_2 \cdot H_2O^+$ is subsequently formed from $O_2 \cdot H_2O^+$ by molecular association with CO_2. A rate coefficient of 2 (− 9) was assumed for reaction (27). To account for the observed amount of $(CO_2)_2O_2^+$ from reaction (26) requires a rate coefficient of $k_{26} \approx 1$ (− 30). The intensity of $O_2 \cdot H_2O^+$ calculated with reaction (27) is still lower than that observed, indicating other sources for $O_2 \cdot H_2O^+$. Such sources are most likely reactions of $CO_2 \cdot H_2O^+$ and $(CO_2)_2 \cdot H_2O^+$ with oxygen.

Carbonyl Sulfide (I.P. 11.17 eV)

The results obtained for this reactant are shown in Figure 8. From the decay of the $CO_2 \cdot CO_2^+$ ion intensity we obtain $k_9 = 1.1$ (− 9). The major product ion is COS^+, so that charge transfer is the dominant process. The solid lines in Fig. 8 were calculated on the basis of the reaction scheme

$$CO_2 \cdot CO_2^+ + COS \xrightarrow{a} COS^+ + 2\,CO_2 \quad (90\%),$$
$$\xrightarrow{b} CO_2 \cdot COS^+ + CO_2 \quad (10\%), \quad (9)$$

$$CO_2 \cdot COS^+ + COS \rightarrow (COS)_2^+ + CO_2\,, \quad (28)$$

$$COS^+ + COS + CO_2 \rightarrow (COS)_2^+ + CO_2 \quad (29)$$

with the rate coefficients $k_{28} = 3$ (− 10) and $k_{29} = 6.5$ (− 27). We cannot exclude that a portion or even all of the $CO_2 \cdot COS^+$ ion intensity derives from the association reaction

$$COS^+ + 2\,CO_2 \rightarrow CO_2 \cdot COS^+ + CO_2\,. \quad (30)$$

If COS^+ were the sole reaction product from reaction (9), rate coefficients of $k_{30} = 2$ (− 30) and $k_{28} = 5$ (− 10) would be required to reproduce the $CO_2 \cdot COS^+$ ion intensity. The major route of $(COS)_2^+$ ion formation in this case is still reaction (29) with $k_{29} = 3.6$ (− 27). The same value was obtained also at 0.3 torr. The high rate coefficient

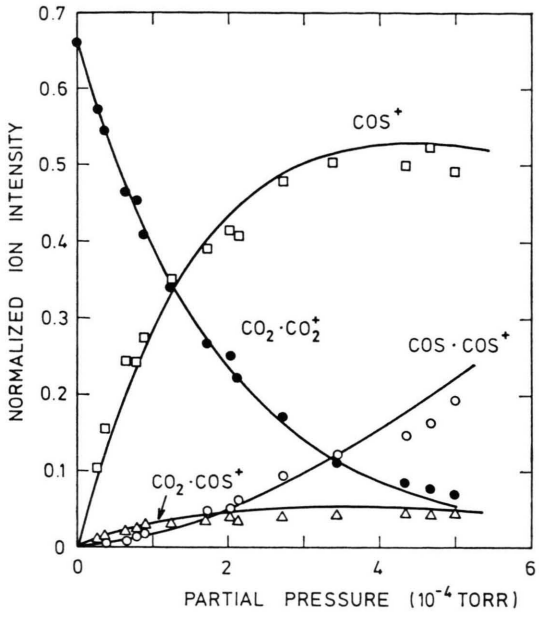

Fig. 8. Reactant and product ion intensities for the reaction of CO_2 dimer ions with carbonyl sulfide. Solid lines were calculated as described in the text.

for reaction (29) is not surprising in view of the dipole forces dominating the interaction of any ion with COS. This case reaction is thus different from the association of N_2O^+ with N_2O discussed above, where dipole forces are of minor significance.

Acetylene (I.P. 11.40 eV)

Results for this reactant are shown in Figure 9. The rate coefficient found, $k_{10} = 7.0\ (-10)$, is again somewhat higher than that reported previously by Sieck [2], 4.3 (−10). More significantly, our product distribution is also different. Specifically, $CO_2 \cdot C_2H_2^+$ is found here to be a product, whereas Sieck reports its absence, concluding that charge transfer constitutes the only product channel. His conclusion will be correct if $CO_2 \cdot C_2H_2^+$ is formed entirely by association of $C_2H_2^+$ with CO_2. Consider the reaction sequence:

$$CO_2 \cdot CO_2^+ + C_2H_2 \xrightarrow{a} C_2H_2^+ + 2\,CO_2\,, \qquad \xrightarrow{b} CO_2 \cdot C_2H_2^+ + CO_2\,, \quad (10)$$

$$C_2H_2^+ + 2\,CO_2 \rightarrow CO_2 \cdot C_2H_2^+ + CO_2\,, \quad (31)$$

$$C_2H_2^+ + C_2H_2 \rightarrow \text{products}, \quad (32)$$

$$CO_2 \cdot C_2H_2^+ + C_2H_2 \rightarrow (C_2H_2)_2^+ + CO_2\,. \quad (33)$$

Two limiting cases may be distinguished depending on whether $CO_2 \cdot C_2H_2^+$ is formed mainly via reaction (10b) or via reaction (31). In the first case

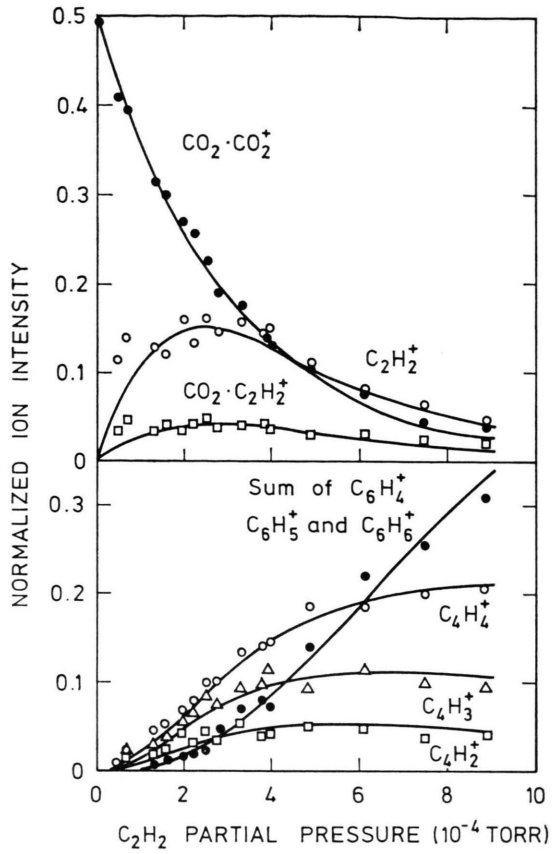

Fig. 9. Reactant and product ion intensities for the reaction of CO_2 dimer ions with acetylene. Lower part shows the direct products, upper part the secondary products. Solid lines were calculated as explained in the text.

when $CO_2 \cdot C_2H_2^+$ derives solely from reaction (10b), the data in Fig. 9 are well reproduced with $k_{10b}/k_{10} = 0.23$, $k_{32} = 1.4\ (-9)$ and $k_{33} = 1.0\ (-9)$, taking $\mu_{88}/\mu_{26} = 0.746$. The corresponding channel probability for charge transfer is 0.77. This value clearly provides a lower limit. In the second case we assume that the probability for charge transfer is unity and all of the $CO_2 \cdot C_2H_2^+$ ion intensity derives from reaction (31). In this case, the data in Fig. 9 can again be reproduced well, if one takes $k_{31} = 4\ (-30)$, $k_{32} = 1.6\ (-9)$ and $k_{33} = 3\ (-10)$. The value for k_{31} lies in the range of values found for other association reactions with CO_2, but it is an upper limit. The value for k_{33} in this case is surprisingly low.

Practically all known rate coefficients for reactions with acetylene are close to the Langevin limit [20]. The Langevin value for reaction (33) is 9.8 (−10) and the rate coefficient $k_{33} = 1.0\ (-9)$ derived from

case I is in agreement with it. For this reason it appears reasonable to assign the greater portion of $CO_2 \cdot C_2H_2^+$ formation to reaction channel (10b).

In both the limiting cases for $CO_2 \cdot C_2H_2^+$ formation the follow-on product of reaction (33), $(C_2H_2)_2^+$ constitutes a minor portion of total $(C_2H_2)_2^+$ produced. In case 1 it provides about 3%, in case 2 it provides 20% of total $(C_2H_2)_2^+$. Most of the $(C_2H_2)_2^+$ is formed in reaction (32). This reaction is known to proceed by three channels [20]

$$\begin{aligned} C_2H_2^+ + C_2H_2 &\xrightarrow{a} (C_2H_2)_2^+ , \\ &\xrightarrow{b} C_4H_3^+ + H , \\ &\xrightarrow{c} C_4H_2^+ + H_2 . \end{aligned} \qquad (32)$$

In the low pressure environment of mass spectrometer ion sources and ion cyclotron resonance technique the probability for $(C_2H_2)_2^+$ formation is low [21, 22], less than 5%; the branching ratio for the channels b and c is $k_{32c}/k_{32b} = 0.50 \pm 0.04$ for $C_2H_2^+$ ions produced either by low energy electron impact or photoionisation [20—22]. The present data are best fitted with $k_{32a}/k_{32} = 0.32$, $k_{32b}/k_{32} = 0.43$ and $k_{32c}/k_{32} = 0.25$; the corresponding branching ratio, $k_{32c}/k_{32b} = 0.58$ somewhat higher than the average value given above. It has been shown [23] that this ratio decreases when the electron impact energy is increased from 12 to 16 eV because the $C_2H_2^+$ ions acquire internal excitation energy. The present high value for the branching ratio indicates that the $C_2H_2^+$ involved are not internally excited. If they acquire excess energy in the charge transfer process from $CO_2 \cdot CO_2^+$ they quickly loose it in the high pressure CO_2 environment. It is probable that reaction (32a) occurs by termolecular association. The corresponding rate coefficient $k_{32a} = k_{32a}/n_M = 1.6$ (-26). Similar high values occur also for association reactions of ethylene and propylene ions discussed further below.

As shown in Fig. 9, all three products from reaction (32) undergo further reactions leading to higher condensation products appearing at mass numbers 78, 77 and 76. If we assign for these products the reaction paths

$$(C_2H_2)_2^+ + C_2H_2 + CO_2 \rightarrow (C_2H_2)_3^+ + CO_2 , \qquad (34)$$

$$C_4H_3^+ + C_2H_2 + CO_2 \rightarrow C_4H_3^+ \cdot C_2H_2 + CO_2 , \qquad (35)$$

$$C_4H_2^+ + C_2H_2 + CO_2 \rightarrow C_4H_2^+ \cdot C_2H_2 + CO_2 , \qquad (36)$$

we obtain the rate coefficients given in Table 2.

Ethylene (I.P. 10.45 eV)

Experimental data for the reaction with ethylene are shown in Figure 10. The reaction is rapid with $k_{11} = 1.35$ (-6). An association product with CO_2 is not observed in this reaction anp $C_2H_4^+$ is the only primary product ion. The $C_2H_4^+$ ion undergoes a further reaction with ethylene, the products being the dimer ion $(C_2H_4)_2^+$ and $C_3H_5^+$. Both products were observed previously [22, 24] at low pressures in mass spectrometer ion sources but with different abundances. $C_3H_5^+$ is the major product in low pressure experiments. It results from the bimolecular encounter of $C_2H_4^+$ with C_2H_4 together with smaller amounts of $C_4H_7^+$ [20—22] which is not observed here. $(C_2H_4)_2^+$ is formed by third body association (even at low pressures [22]). A small portion of the ethylene dimer ions react further giving rise to trimeric $(C_2H_4)_3^+$ ions. For simplicity, their intensity is combined with that of $(C_2H_4)_2^+$ in Figure 10. The solid lines shown were calculated on the basis of the reaction scheme

$$C_2H_4^+ + C_2H_4 \rightarrow (C_2H_4)_2^{+*} , \qquad (37)$$

$$(C_2H_4)_2^{+*} \rightarrow C_3H_5^+ + CH_3 , \qquad (38)$$

$$(C_2H_4)_2^{+*} + CO_2 \rightarrow (C_2H_4)_2^+ + CO_2 , \qquad (39)$$

where $k_{37} = 1.8 \cdot 10^{-9}$, $\mu_{88}/\mu_{28} = 0.81$ and the probabilities for $C_3H_5^+$ formation and $(C_2H_4)_2^+$ stabiliza-

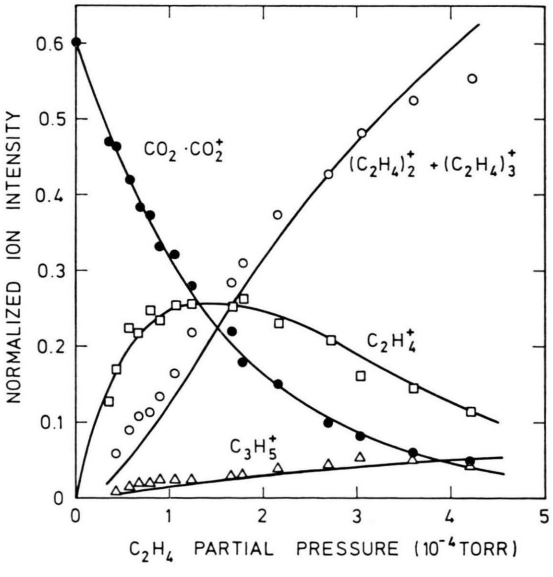

Fig. 10. Reactant and product ion intensities for the reaction of CO_2 dimer ions with ethylene. Solid lines were calculated as explained in the text.

tion are 0.077 and 0.923, respectively. Stabilized ethylene dimer formation occurs with a rate corresponding to a termolecular rate coefficient of 6 (−26) which is in reasonable agreement with the value derived previously by one of us [22], 1.6 (−25). If one assumes that reaction (39) proceeds with the Langevin collision rate, 8.1 (−10), one can calculate the unimolecular rate coefficient for the break-up of $(C_2H_4)_2^+$ to yield $C_3H_5^+$ as $k_{38} = 1.9$ (−6) s^{-1}. It is clear that with increasing pressure this reaction channel will be more and more suppressed.

Propylene (I.P. 9.74 eV)

Results for propylene as a reactant are shown in Figure 11. Only charge transfer and dissociative charge transfer products are observed, namely $C_3H_6^+$ (52%), $C_3H_5^+$ (40%), and $C_3H_4^+$ (8%). The rate coefficient, $k_{12} = 2.0$ (−9) has about twice the Langevin value. If this result is correct it would indicate that charge transfer occurs by a long-range process. The primary products react further with propylene giving rise to a considerable number of secondary products. Rate coefficients for these reactions were obtained from the variation of $C_3H_6^+$, $C_3H_5^+$ and $C_3H_4^+$ ion intensities as a function of propylene pressure as $k_{40} = 2.1$ (−9), $k_{41} = 2.1$ (−9), $k_{42} = 1.6$ (−9). From the product ion distribution at $1 \cdot 10^{-4}$ torr of propylene and the calculated product ion intensities from each of the three secondary reactions we derive the approximate channel probabilities as follows:

$$\begin{aligned}
C_3H_6^+ + C_3H_6 &\xrightarrow{a} C_6H_{12}^+ && (57\%),\\
&\xrightarrow{b} C_4H_7^+ + C_2H_5 && (11\%),\\
&\xrightarrow{c} C_4H_8^+ + C_2H_4 && (19\%),\\
&\xrightarrow{d} C_5H_9^+ + CH_3 && (13\%), \quad (40)\\
C_3H_5^+ + C_3H_6 &\xrightarrow{a} C_6H_{11}^+ && (83\%), \quad (41)\\
&\xrightarrow{b} D_5H_8^+ + CH_3 && (17\%),\\
C_3H_4^+ + C_3H_6 &\rightarrow C_4H_8^+ + C_2H_2 && (100\%). \quad (42)
\end{aligned}$$

The dominant products $C_6H_{11}^+$ and $C_6H_{12}^+$ will be formed by third body association involving CO_2. The corresponding termolecular rate coefficients have values similar to those found for ion association in ethylene (see Table 2). An association product of $C_6H_4^+$ with propylene was not detected. The product distribution for reaction (40) among the channels b, c and d, is approximately 25, 45 and 30 percent, respectively. The ion $C_3H_7^+$, observed in many previous investigations [25–28] of this reaction has not been detected here. The probabilities

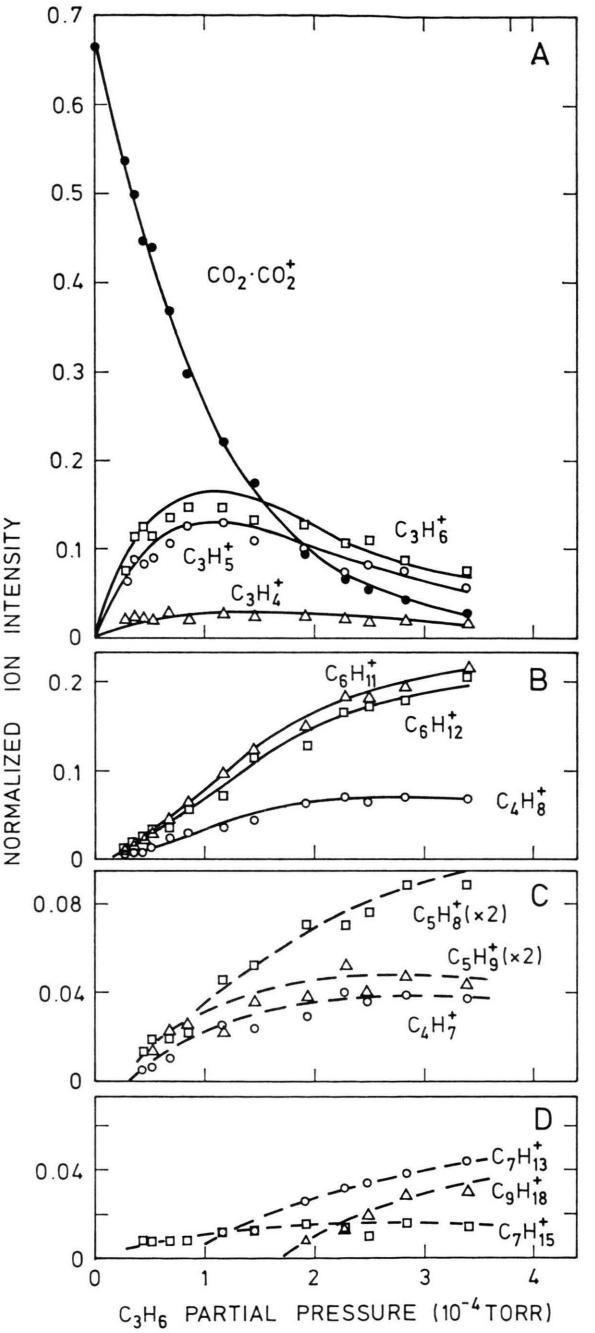

Fig. 11. Reactant and product ion intensities for the reaction of CO_2 dimer ions with propylene. (a) Primary products from the reaction, (b) and (c) secondary and tertiary products. Solid lines were calculated as explained in the text. Dashed lines indicate observed behavior.

for channels (40c) and (40d) are in approximaet agreement with those found previously under conditions of low pressure in photoionisation mass

spectrometry [26] and by ICR technique [27], but our probability for channel (40b) is by a factor of two higher.

When the partial pressure of propylene is increased, higher condensation products appear in low yield at mass numbers 97, 99 and 126. The last one of these corresponds to the trimeric ion $(C_3H_6)_3^+$. If the reaction for its formation is third body assisted association of $C_6H_{12}^+$ with propylene, a rate coefficient of $k_{43} = 8.2$ (−26) will be required to yield the observed ion intensity.

Ammonia (I.P. 10.17 eV)

Experimental results for the reaction of CO_2 dimer ions with ammonia are shown in Figure 12. The rate coefficient is $k_{13} = 6.0$ (−10). Both NH_3^+ and $CO_2 \cdot NH_3^+$ appear as initial products and if these are assigned to result from the reaction

$$CO_2 \cdot CO_2^+ + NH_3 \xrightarrow{a} NH_3^+ + 2\,CO_2\,, \quad (13)$$
$$\xrightarrow{b} CO_2 \cdot NH_3^+ + CO_2$$

each of the products will be formed with a channel probability of approximately 50%. As in the case of acetylene it is possible, however, that charge transfer via channel (13a) is dominant and that $CO_2 \cdot NH_3^+$ is formed subsequently by third body association of NH_3^+ with CO_2

$$NH_3^+ + 2\,CO_2 \rightarrow CO_2 \cdot NH_3^+ + CO_2\,. \quad (44)$$

In this case a rate coefficient $k_{44} = 2$ (−29) is required to yield the observed $CO_2 \cdot NH_3^+$ ion intensity. This value provides an upper limit. From the behaviour of NH_3^+ and $CO_2 \cdot NH_3^+$ ion intensities shown in Fig. 12 it is apparent that both ions undergo subsequent reactions

$$NH_3^+ + NH_3 \rightarrow NH_4^+ + NH_2\,, \quad (45)$$

$$CO_2 \cdot NH_3^+ + NH_3 \xrightarrow{a} NH_4^+ + NH_2 + CO_2\,,$$
$$\xrightarrow{b} CO_2 \cdot NH_4^+ + NH_2\,, \quad (46)$$

$$NH_4^+ + NH_3 \rightleftarrows NH_3 \cdot NH_4^+\,. \quad (47)$$

The assumption that $CO \cdot NH_4^+$ is formed in reaction (46b) is made here merely for simplicity. It is clear that this ion can arise also from the association of NH_4^+ with CO_2. Reaction (45) has been investigated previously [29] and rate coefficients clustering around a value of 1.5 (−9) were obtained. The equilibrium (47) has also been studied previously [30]. We have not specifically considered it, but rather have added the observed small intensities of $NH_3 \cdot NH_4^+$ to that of NH_4^+. If reaction (13) is assumed to occur as written with each channel contributing 50% to the formation of the products, the data in Fig. 12 are best reproduced using $k_{45} = 1.3$ (−9), $k_{46} = 8.5$ (−10), $k_{46a}/k_{46} = 0.8$ and $\mu_{88}/\mu_{17} = 0.646$. The solid lines in Fig. 12 were calculated with these values. The rate coefficient for reaction (45) required to fit the data is in reasonable agreement with the previous determinations [29]. If charge transfer were the only mode of reaction (13) and all of the $CO_2 \cdot NH_3^+$ ion intensity were due to reaction (44), we would essentially require the same rate coefficients for reaction (45) and (46) to fit the experimental data.

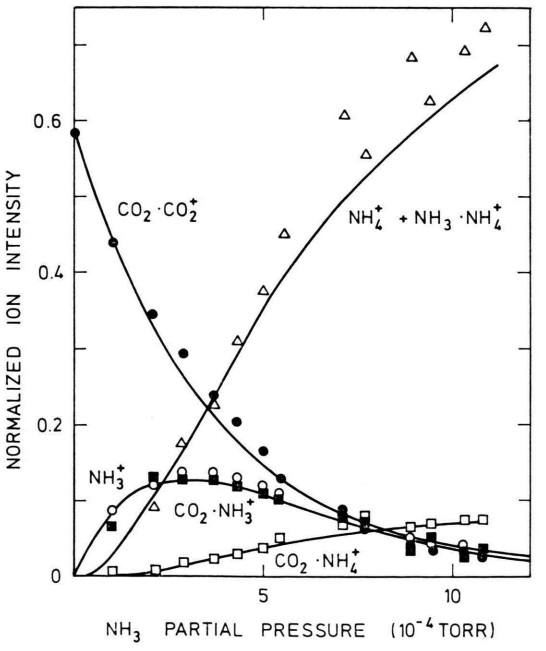

Fig. 12. Reactant and product ion intensities for the reaction of CO_2 dimer ions with ammonia. Solid lines were calculated as explained in the text.

Methylamine (I.P. 8.97 eV)

The reaction of this compound with $CO_2 \cdot CO_2^+$ ions was found to be unexpectedly slow, $k_{14} = 1.7$ (−12). Product ions occurred at mass numbers 17, 18, 32, 61 and 76. They are tentatively identified as NH_3^+ (24), NH_4^+ (9), $CH_3NH_3^+$ (20), $CO_2 \cdot NH_3^+$ (24), and $CO_2 \cdot CH_3NH_3^+$ (23) where the number in parentheses indicates approximate percentage abundances. Since the investigation of such slow

reactions requires fairly high reactant partial pressures, it is possible that the observed decrease of $CO_2 \cdot CO_2^+$ ion intensity with increasing reactant concentration and the associated products are due to a reaction with the precursor ion CO_2^+ rather than reaction (14). We have looked at the reaction of CO_2^+ with methylamine at a total pressure of 0.28 torr where, as Fig. 1 shows, CO_2^+ is still the major ion in the reaction chamber. To our surprise we found that also the reaction $CO_2^+ + CH_3NH_2$ is slow, so that an interference of this reaction with reaction (14) at the higher pressure of 0.85 torr can be precluded. If one assumes a $CO_2 \cdot CO_2^+$ ion electron recombination energy close to that for CO_2^+ (vide infra), the only exoergic reaction channels available for reaction (14) are

$$\begin{aligned} CO_2 \cdot CO_2^+ + CH_3NH_2 & \\ \xrightarrow{a} CH_3NH_2^+ + 2\,CO_2 & \quad -4.82\,\text{eV}, \\ \xrightarrow{b} NH_2^+ + CH_3 + 2\,CO_2 & \quad -1.23\,\text{eV}, \\ \xrightarrow{c} NH_4^+ + CH + 2\,CO_2 & \quad -0.86\,\text{eV}. \end{aligned} \tag{14}$$

The product ion $CH_3NH_2^+$ is known to react rapidly [31] with methylamine yielding $CH_3NH_3^+$ and subsequently by reaction with CO_2 to form the association product $CO_2 \cdot CH_3NH_3^+$. The ion $CH_3NH_3^+$ may also arise from NH_4^+ by proton transfer [32] to CH_3NH_2 and this reaction will be fast. The fact that NH_4^+ is observed as a product while $CH_3NH_2^+$ is not, may be an indication for the insignificance of reaction channel (14a). The ion NH_2^+ is not observed but this ion can enter into three exoergic and probably rapid reactions with methylamine.

$$\begin{aligned} NH_2^+ + CH_3NH_2 & \\ \xrightarrow{a} CH_3NH_2^+ + NH_2 & \quad -2.43\,\text{eV}, \\ \xrightarrow{b} NH_3^+ + CH_2NH_2 & \quad -1.67\,\text{eV}, \\ \xrightarrow{c} CH_3NH_3^+ + NH & \quad -2.81\,\text{eV}. \end{aligned} \tag{48}$$

The first and the last reaction channels ultimately lead to $CH_3NH_3^+$ and its association product with CO_2. The reaction channel (48b) appears to provide the only exoergic route to NH_3^+ production. It is amazing that this ion can persist in the presence of methylamine with the observed intensity in view of the fact that both charge transfer and hydrogen abstraction from CH_3NH_2 are energetically favorable and are probably fast [33]. The observation of NH_3^+ leads us to believe that reaction channels (14b) and (48b) are important in the $CO_2 \cdot CO_2^+ + CH_3NH_2$ reaction system, but the determination of channel probabilities for the formation of the various products from reaction (14) will require additional studies on the secondary reactions in this system.

Nitric Oxide (I.P. 9.25 eV)

The reaction with NO is also extremely slow. The decrease of $CO_2 \cdot CO_2^+$ ion intensity indicates a rate coefficient $k_{15} = 4.5\,(-12)$ but this is a definite upper limit, because the reaction of CO_2^+ with NO is known to be much faster; the associated rate coefficient has a value [34] of $1.2\,(-10)$. When this reaction is taken into account one finds that essentially all of the $CO_2 \cdot CO_2^+$ intensity decrease is due to the reaction of the CO_2 precursor ion. The value given in Table 1 for k_{15} constitutes a conservative upper limit. We can offer no reasons for the lack of reactivity of NO towards $CO_2 \cdot CO_2^+$ particularly when compared to the normal rate of the $CO_2^+ + NO$ reaction.

Conclusions

Charge transfer occurs as a prominent reaction mode in practically all reactions studied provided it is energetically allowed. Molecular displacement (switching) reactions appear to occur also in several cases albeit with lesser probability. Only in one reaction, that of $CO_2 \cdot CO_2^+$ with O_2, has the extent of molecular displacement been determined with some confidence. In general, the switching product can also arise from termolecular association of the charge transfer product with CO_2. Most of the associated rate coefficients are not known. For O_2^+, however, it was possible to determine the rate coefficient in an independent experiment. Except for the reactions with CH_3NH_2 and NO the rate coefficients have values in accordance with or somewhat smaller than ADO theory [14]. Rate coefficients for reactions of CO_2^+ with the same reactants, where known (CH_4 [35], H_2O [17], O_2 [36], NO [34]), have similar values, an effect of dimerization of CO_2^+ in these cases is not apparent. The major exception occurs for nitric oxide.

The dissociation energy of the $CO_2 \cdot CO_2^+$ ion and its heat of formation are not well known. The electron ion recombination energy of $CO_2 \cdot CO_2^+$ is certainly greater than the ionization potential of N_2O, since charge transfer to this molecule is efficient, and it must be smaller than the ionization

potential of CO_2 or $CO_2 \cdot CO_2^+$ would be unstable. These limits [33], $12.89 < RE(CO_2 \cdot CO_2^+) < 13.79$ eV lead to dissociation energies in the range $O < D(CO_2 - CO_2^+) < 0.9$ eV corresponding to 0—86.7 kJ/mol. The equivalent range for the heat of formation of $CO_2 \cdot CO_2^+$ is 452.5—539.2 kJ/mol. The lack of suitable reactants having ionisation potentials between 12.9 and 13.8 eV makes it difficult to narrow this range. The observation that with propylene as a reactant dissociation charge transfer products are observed whereas with ethylene they are not may indicate a lower upper limit to RE $(CO_2 \cdot CO_2^+)$. The appearance potentials [33] for $C_3H_5^+$ and $C_3H_4^+$ from C_3H_6 are 11.88 and 12.3 eV, respectively, i.e. well below the ionisation potential of $(N_2O^+$. The appearances potentials [33] for $C_2H_2^+$ and $C_2H_3^+$ from C_2H_4 are 13.13 and 13.25 eV, respectively. Since neither of these ions nor conceivable follow-on product ions were observed it appears that RE $(CO_2 \cdot CO_2^+)$ is equal to or less than 13.13 eV. The above range of $CO_2 \cdot CO_2^+$ dissociation energies is thus narrowed to 63.5—86.7 kJ/mol, corresponding to values in the range 452.5—475.7 kJ/mol for the heat of $CO_2 \cdot CO_2^+$ formation.

We are grateful for a research fellowship granted to A. B. Rakshit by the Max-Planck-Gesellschaft.

[1] V. Nestler, B. Betz, and P. Warneck, Ber. Bunsenges. Phys. Chem. **81**, 13 (1977).
[2] L. W. Sieck, Int. J. Chem. Kinet. **10**, 335 (1978).
[3] J. M. Schildcrout, J. G. Collins, and J. L. Franklin, J. Chem. Phys. **52**, 5767 (1970).
[4] A. R. Anderson and P. A. Dominey, Radiat. Res. Rev. **1**, 269 (1968); D. A. Parkes, J. Chem. Soc Fadaray I **69**, 198 (1973); C. Willis and A. W. Boyd, Int. J. Radiat. Phys. Chem. **8**, 71 (1976); A. J. Wickham, J. V. Best, and C. J. Wood, Int. J. Radiat. Phys. Chem. **10**, 107 (1977).
[5] R. C. Whitten, I. G. Popoff, and J. S. Sims, Planet. Space Sci. **19**, 243 (1971); L. W. Sieck, R. Gordon Jr., and P. Ausloos, ibid **21**, 2 P 39 (1973).
[6] J. L. McCrumb and P. Warneck, J. Chem. Phys. **66**, 5416 (1977).
[7] D. Smith, N. G. Adams, and T. M. Miller, J. Chem. Phys. **69**, 308 (1978); W. Lindinger, F. C. Fehsenfeld, A. L. Schmeltekopf, and E. E. Ferguson, J. Geophys. Res. **79**, 4753 (1974).
[8] M. Saporoschenko, Phys. Rev. **A 8**, 1044 (1973).
[9] H. W. Ellis, R. Y. Pai, R. Gatland, E. W. McDaniel, R. Wernland, and M. J. Cohen, J. Chem. Phys. **64**, 3935 (1976).
[10] J. T. Moseley, R. A. Bennett, and J. R. Peterson, Chem. Phys. Lett. **26**, 288 (1974).
[11] J. F. Paulson, F. Dale, and R. F. Mosher, Nature London **204**, 377 (1964); L. W. Sieck and R. Gordon Jr., J. Res. Nat. Bur. Stand. **78 A**, 315 (1974).
[12] G. P. Smith, P. C. Cosby and J. T. Moseley, J. Chem. Phys. **67**, 3818 (1977).
[13] J. L. McCrumb and P. Warneck, J. Chem. Phys. **67**, 5006 (1977).
[14] T. Su and M. T. Bowers, J. Chem. Phys. **58**, 3027 (1973); Int. J. Mass Spectrom. Ion Phys. **12**, 347 (1973).
[15] L. W. Sieck, R. Gordon Jr., P. Ausloos, and S. G. Lias, Rad. Res. **56**, 441 (1973).
[16] A. G. Harrison and A. S. Blair, Int. J. Mass Spectrom. Ion Phys. **12**, 175 (1973).
[17] Z. Karpas, V. G. Anicich, and W. T. Huntress Jr., Chem. Phys. Lett. **59**, 84 (1978).
[18] A. B. Rakshit, Chem. Phys. Lett., in press.
[19] N. G. Adams, D. K. Bohme, D. B. Dunkin, F. C. Fehsenfeld, and E. E. Ferguson, J. Chem. Phys. **52**, 3133 (1970).
[20] L. W. Sieck and S. G. Lias, J. Phys. Chem. Ref. Data **5**, 1123 (1976).
[21] J. K. Kim, V. G. Anicich, and W. T. Huntress Jr., J. Phys. Chem. **81**, 1798 (1977), and references cited therein.
[22] P. Warneck, Ber. Bunsenges. Phys. Chem. **76**, 421 (1972).
[23] R. M. O'Malley and K. R. Jennings, Int. J. Mass Spectrom. Ion Phys. **2**, 257 (1969).
[24] F. H. Field, J. Amer. Chem. Soc. **83**, 1523 (1961).
[25] F. P. Abramson and J. H. Futrell, J. Phys. Chem. **72**, 1994 (1968).
[26] L. W. Sieck and S. K. Searles, J. Amer. Chem. Soc. **92**, 2937 (1970).
[27] J. M. S. Henis, J. Chem. Phys. **52**, 282 (1970).
[28] A. G. Harrison, G. P. Nagy, M. S. Chin, and A. A. Harod, Int. J. Mass Spectrom. Ion Phys. **9**, 287 (1972).
[29] W. T. Huntress Jr. and R. F. Pinizzotto Jr., J. Chem. Phys. **59**, 4742 (1973), and references contained therein.
[30] F. C. Fehsenfeld and E. E. Ferguson, J. Chem. Phys. **59**, 6272 (1973).
[31] L. Hellner and L. W. Sieck, Int. J. Chem. Kinet. **5**, 177 (1973).
[32] R. Yamdagni and P. Kebarle, J. Amer. Chem. Soc. **95**, 3504 (1973).
[33] H. M. Rosenstock, K. Draxl, B. W. Steiner, and J.T. Herron, Energetics of Gaseous Ions, J. Phys. Chem. Ref. Data **6**, Suppl. 1 (1977).
[34] F. C. Fehsenfeld, D. B. Dunkin, and E. E. Ferguson, Planet. Space Sci. **18**, 1267 (1970).
[35] S. L. Chong and J. L. Franklin, J. Chem. Phys. **54**, 1487 (1971); S. F. Kasper and J. L. Franklin, J. Chem. Phys. **56**, 1156 (1972); A. G. Harrison and A. S. Blair, Int. J. Mass Spectrom. Ion Phys. **12**, 175 (1973).
[36] W. Lindinger, F. C. Fehsenfeld, A. L. Schmeltekopf, and E. E. Ferguson, J. Geophys. Res. **79**, 4753 (1974).